Performance Analysis of image compression in MRI Brain Images using ROI and Non ROI Coding Techniques

Sr. J. Rani[1], Dr.G. Glorindal[2] & Dr. Ignatius A Herman[3]

[1]Research scholar, St. Eugene University, Zambia. E-mail: ranij79@gmail.com

[2]Department of CS & IT, DMISIBU Lilongwe, Malawi. E-mail: glorygj@yahoo.com

[3]Director of Education, DMI Group of Institutions, Africa.

Abstract

The growing demand for medical image storage and transmission has resulted in a shortage of memory and bandwidth. Compression was used to find these issues. Clinical image compression is used to improve image quality, reduce bit rate, increase compression efficiency for storage and transmission, and reduce cost. MRI images are quite clinical. To store and transmit thousands of MRI pictures, you need a lot of storage space and bandwidth. Thus, high-quality MRI image compression is more research focused. Many Compression strategies for MRI with low compression rate cause loss of data on lesions, and lead to misdiagnose. This research proposed several MRI image compression methods. Our main goals are to provide more compressed clinical images, encourage early location and finding followed by therapy using multi-resolution compression technology. A two-dimensional (2D) picture arrangement is created by first converting 3D MRI scans into 2D images. Then range and area blocks are arranged by 3D object's spatio-temporal similarity. In addition, the proposed technique uses wavelet transform and MRG algorithm to analyse the performance of wavelet contains transformation, quantization, and entropy coding to compress the most significant piece of ROI using DWT and s. It compresses non-ROI using DCT and MHE (merging based Huffman encoding). Finally, residual compensation is used to provide good decompression quality MRI compression.

Keywords: Image Processing, MRI, Compression, Images.

1. Introduction

An image is the most popular and often used way to present data. In general, is of significant importance in the clinical arena as assurance and treatment of practically any disease. An image is created by collections of pixels that are associated with one another. These findings identify three redundancies which are essential to how much storage is required and how fast

transmission speeds are. We include temporal, spatial, and spectral redundancy in our algorithm. Redundancy is eliminated when images are compressed. There are a variety of ways to still image compression, and many articles have been written about the issue. These estimates are based on picture compression that is lossy and lossless. To the layperson, lossy compression is commonly known as file reduction. There is no concern about image quality or content while using lossless compression. The lossless compression methods of run-length encoding, chain codes, and deflate all utilise entropy encoding, run-length encoding, and compression coding. Redundant data is taken out of the picture using lossy compression, which creates content that is needed. The sort of compression that is based on human vision is known as ostensibly lossless compression (OLC). Most people tend to employ the DCT, fractal compression, and the newly implemented wavelet transform when using VLC. Three sorts of redundancy are typically present in an automated image: psycho-visual, spatial, and coding [1]. The image is packed using these redundancies. JPEG is a popular image compression method for clinical photographs that combines DCT and Huffman coding. Wavelets [discrete wavelet transform (DWT)] have recently achieved epic wins in the realm of picture compression [2]. Aspect ratio coding (ACR) is employed in lossless compression [3]. There are two clear and free aspects to lossless compression: showing and coding [3]. Wavelet transform, VQ, neural association, and various encoding techniques are commonly used for image compression [4]. Using video coding techniques like H.264/MPEG-4 AVC [5] or the more recent H.265/MPEG-H HEVC [6] to store 3D and 4D clinical picture files has been suggested [7]. Furthermore, the expanding accessibility and use of electronic imaging relieves concern for a well-organized image compression structure and for enhancing image quality [8]. However, despite high compression rates, the accommodation of converted images is dependent on certain basic properties of the parent image, which should be ensured after the compression cycle [9].

This research examines clinical picture compression utilising wavelet transform and modified district developing (MRG) [25]. We offered a whole report on the use of wavelet includes transform, quantization, and entropy coding for clinical image compression. Distinct wavelet transform and lifting plans are combined. Some of the quantitative and emotional image gauges are: compression rate or contact rate, bits per pixel size (BPP), PSNR, most notable mix-up, mean square Error (MSE), L2-Norm size. We initially divide the image into two segments: interest (return on investment) and non-interest (non-return on investment). Starting there, we set

parcelling in progressive tree (SPIHT) encoding for the principal return on initial capital investment [26]. As a result, we pack the non-return on initial capital investment (NICI) using DCT and MHE. That's when we combine money invested with non-return on initial capital. Finally, we receive the packed image and later determine the compression ratio to test the proposed approach. The decompression cycle uses the opposite cycle. The following are the exploration's primary responsibilities:

2. Proposed Work

In telemedicine, as well as in many other cases, lossless compression is unable to achieve the steady-image transmission criteria. A dedication to lossy compression is a must. At the expense of image division data, a constant transmission objective piece rate is imported. Image compression innovation is enabling the development of a critical capability for telemedicine and clinical imaging applications with high-limit requirements. Constructed in such a way that clinical images can be compressed at a high compression ratio and without loss of quality. The region of interest (ROI) compression technique has developed into a notable advancement in specialised picture compression, being frequently employed in distributed writings. The return on investment compression technique has developed into a substantial improvement in the field of specialized picture compression, covering a wide range of adapted compositions.

2.1. ROI Coding

The return on initial capital investment coding (ROIC) method separates an image into two parts: the return on investment (ROI) portion and the foundation portion. Bruckmann et al. [10] examined lossy compression in explicit image compression using wavelet transforms and JPEG. Wavelet transform compression is superior to JPEG, according to preliminary studies. They devised a method for removing coefficient covers based on the return on investment (ROI) provided by JPEG2000. To achieve complete ROI coding, we adjusted the wavelet coefficients using separate sub-bunches. Zhang et al. [3] proposed a neural association based classification technique. Hosseini et al. [12] demonstrated how to estimate the CVQ for MRI image compression using a setting-based approach. The calculation separated the ROI from the background in a photo using the region-creating method, and then packed the two segments independently using the proposed CVQ plan. Sophia and Anitha's [13] computation compresses some image segments losslessly using run-length coding, Huffman coding, or math coding,

while compressing the BG lossily by vector quantization. Kaura and Wasson [14] offer a method for performing lossless compression and lossy tension on BG that makes advantage of fractal computation. Irritation and other flaws in the clinical image are more symptomatic of a more serious condition. Schelkens et al. [15] extended the adaptability of the embedded code stream by the implementation of a multi-return on initial capital investment (MCI) general display. Sridhar [16] offered a ROI calculation or clinical images in which the irritated zone was considered the return on initial capital investment, and the incorporating painful (often feeble district) "Multi-ROI clinical picture compression computation with tense component protection", [17]. The BG was compressed using SPIHT and the supporting image edge information was removed using Watchful Overseer.

Firoozbakht et al. developed a strategy based on setup and multiple-ROI coding. The ROIs calculated included an essential ROI (the location of the vascular stenosis), an optional ROI (the location of other important veins), and BG. The primary ROI should have been physically chosen, whereas the secondary ROI should have been calculated using the local development technique. Rapestaetal's need-based ROI coding approach is a combination of Bartrina and Rapestaetal's approaches. [19] coded various ROIs for a variety of purposes using a simple and effective ROI coding rate assignment mechanism. To eliminate connections in stereoscopic clinical imaging, multidimensional wavelet modifications are widely used. Agrafiotis et al. [20] extended the three-dimensional SPIHT approach to allow for three-dimensional ROI coding. Wang and Cuhadar [21] proposed employing a three-dimensional tree structure to accomplish multiple returns on investment and multiple quality controls in clinical imaging. Victor et al. [22], on the other hand, proposed an improved three-dimensional flexible compression approach for clinical photographs.

Nguyen et al. [23] proposed a method for compressing data that is efficient and is based on movement pay. The proposed work uses a 3D compression approach based on progressive vector quantization to compress the pre-prepared material. Sanchez [24] proposed a technique for compressing 3D clinical images using lossy compression. Joint source channel coding allowed for the creation of varied three-dimensional ROIs to accommodate rising remote transmission requirements. According to Sid Ahmed et al. [27], a reversible discrete cosine change encoder could be used (RDCT). The redesigned structure was closely coupled with a zero tree wavelet encoder (LEZW).

2.2. Non-ROI Coding

The ROI coding method divides an image into two components: the ROI and the foundation (BG). These experiments compressed photos explicitly using wavelet transformations and JPEG. In preliminary testing, wavelet compression outperforms JPEG. They developed a coefficient cover removal coding algorithm based on the ROI of JPEG2000. To complete the ROI coding, sub-bunched wavelet coefficients were shifted. Zhang et al. [3] suggested classifiers based on neural associations. Hosseini and Naghsh Nilchi proposed a setting based CVQ estimate for MRI image compression (12). Following the region-creation method, the two sections were packed individually using the proposed CVQ strategy. These calculations compress some image segments losslessly using, arithmetic coding, Huffman coding or run-length coding whereas vector quantization compresses the BG lossily. Kaura and Wasson [14] use fractal computations to generate lossless compression and lossy tension on BG. Irritation and other clinical abnormalities are more alarming indicators. Schelkens et al. [15] extended the adaptability of the embedded code stream by the implementation of a multi-return on initial capital investment (MCI) general display. Sridhar [16] created a "Multi-ROI clinical image compression computation with tense component protection" that uses the irritated zone to calculate the return on initial capital investment. To eliminate supporting image edge information, the BG was compressed using SPIHT and Watchful Overseer. Firoozbakht et al. proposed a method for setting up and coding multiple ROIs. We estimated an essential ROI (the location of the vascular stenosis), an optional ROI (additional relevant vein locations), and BG. The primary ROI should have been physically selected, whereas the secondary ROI should have been calculated using the local development technique. Rapestaetal's ROI coding approach is based on the Bartrina-part. [19] may use this fundamental concept to code numerous ROIs for a variety of purposes. Multidimensional wavelet modifications are frequently employed in stereoscopic clinical imaging to eliminate connections. Agrafiotis et al. extended 3D SPIHT coding. In order to attain multiple ROI and quality controls, Wang and Cuhadar [21] proposed employing a three-dimensional tree structure for clinical imaging. The adjustable three-dimensional compression method described by Victor et al. enables more advanced clinical imaging. They studied an efficient compression strategy based on mobility pay in the work by Nguyen et al. [23]. The application uses a three-dimensional compression algorithm that uses progressive vector quantization to compress pre-prepared material. Using lossy compression to save three-

dimensional clinical images, Sanchez proposed lossy compression [24–26]. The use of joint source channel coding enabled the creation of additional three-dimensional ROIs for distant transmission. Ahmed et al., proposed the reversible discrete cosine change encoder (RDCT). The redesign structure was securely connected with a zero tree wavelet encoder (LEZW).

2.3. Fractal MRI Image Compression Based on Sequence Image

The information added to a 2D image is in the form of a 3D data square. This is done by reducing images to 2D progressive ones, which can be used in designs that utilize data blocks. To begin, the compressed image is divided into NXN pixel blocks of specified size. Reach blocks are images that do not overlap and spread the image completely (which means R block). The image to be encoded is splitted into 2N X 2N area blocks (D squares), which may span the full image. The D square is exhibited in the middle of four consecutive pixels before encoding, its size lowered to match the R block. The calculated centre value of the investigated D square undergoes eight equidistant transforms, resulting in a codebook. Find the codebook's best R block organizing D square. R = s • D + o • 1 is then used to approximate it. D square's separation and splendor adjustment components are denoted by 1 and s, o, respectively. Otherwise, it is depending on the progression image.

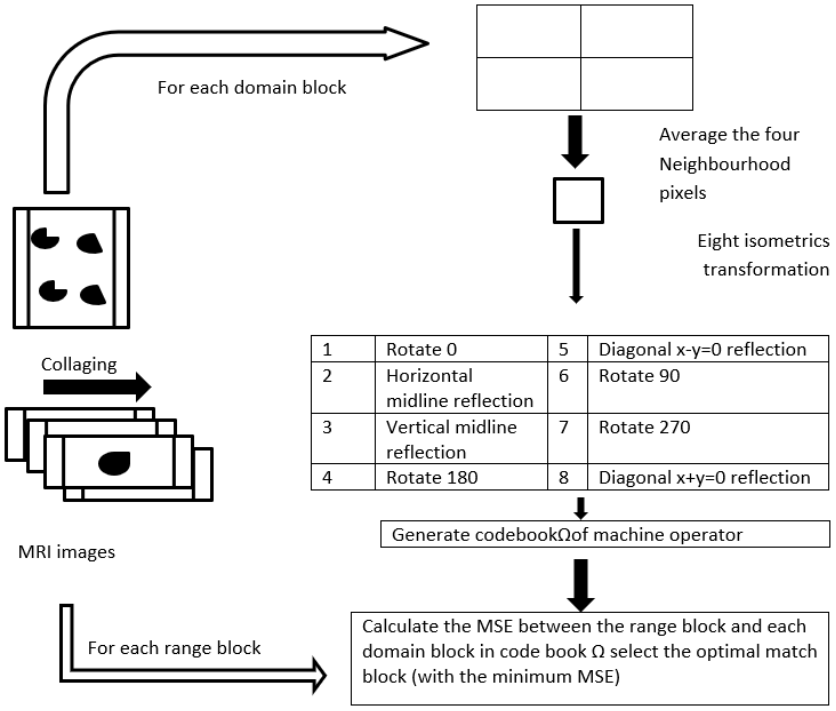

Fig.1. Flow diagram of the sequence image based fractal MRI image compression

Steps Followed for the proposed compression algorithm:

MRI picture F of size M. File dx, dy, t, s, o.

First, MRI image F is partitioned into a fixed block partition (R block) which has a N ×N size but which is not overlapping. Second , A window size of δθ (where θ is the step size) is used to shift the 2N × 2N window by an amount δ in either direction of horizontal and vertical side of the image, then the windowed blocks created after each shift compose a domain block (D block).

Third: The average of all D block samples are calculated and then applied with eight equidistant transformations on the codebook to obtain a codeword.

Fourth: Find the best matching block D 0 j that satisfies in codebook Ω, For an arbitrary range block Ri,

$$d\left(R_i, W_i(D_j)\right) = \min \text{ll } R_i - (s_i.(t_k\ (D_k) + o_i\ )\quad ^2$$

In this domain block after average sampling. $t_k \in \{t1, \cdots, t8\}$ are eight isometric transforms. s_i and oi are contrast factor and luminance factor of gradation transformation, respectively, and are calculated according to Equations given below is the total number of pixels, and r_p, d_p are the p^{th} pixel values of range block and domain block, respectively.

$$s = \frac{\sum_{p=1}^{n} d_p r_p - \sum_{p=1}^{n} d_p \sum_{p=1}^{n} r_p}{n\sum_{p=1}^{n} d_p^2 - \left(\sum_{p=1}^{n} d\right)^2}$$

$$o = \frac{1}{n}\left[\sum_{p=1}^{n} r_p - s\sum_{p=1}^{n} d_p\right]$$

2.3.1. Classification of MRI Image Sub-Blocks

In order to reduce the size of the sequence image, the following steps are taken: Image F (MxM) from MRI as input A file with the following fractal encoded data:

$$\begin{cases} h_{A1} = \frac{1}{n}(h_{11} + h_{21} + \cdots + h_{n1}) \\ h_{A2} = \frac{1}{n}(h_{12} + h_{22} + \cdots + h_{n2}) \\ h_{A2^b} = \frac{1}{n}\left(h_{12^b} + h_{22^b} + \cdots + h_{n2^b}\right) \end{cases}$$

Secondly, domain block $D_j^{'} = \left(h_{j1}, h_{j2}, \ldots h_{j2^b}\right)$is fetched out one by one from domain block set $\left\{D_1^{'}, D_2^{'}, \ldots \ldots, D_n^{'}\right\}$. The distance D_A which the cluster center is calculated according to Eq.1

dis……..(1)

Again, let the initial threshold be σ_p (σ_p is the median of threshold sequence $\{\sigma_i\}$, and the i[th] class domain block C_{Di}i corresponds to the threshold σD_i = σp. Then, the domain blocks whose distance is less than or equal to σD_i is divided into the i[th] class C_{D_i}.

Suppose the class C_{Di} contains a number of domain blocks of ω_i. If ωi »/m, the threshold is adjusted to $\sigma_{Di} = \sigma_{p-1}$, where $\sigma_{p-1}$is an order of magnitude smaller than σp. And so on until ω_i − (M−2N δ + 1)2 /m $w_i - \frac{M-2N}{\delta} + \frac{1}{m} \vee \leq 10$ or $w_i - w_i' \vee \geq 10^{\left(log_{10} w_i - 1\right)}$

Similarly, if $w_i \ll 1$), the threshold σ_p is adjusted to σ_{p+1}. Until $w_i - \frac{M-2N}{\delta} + 1 \quad ^2/m \vee \leq 10^{\left(log|10^{w_i-1}\right)}$ or $w_i - w_i' \vee \geq 10^{\left(log|10^{w_i-1}\right)}$. Adjustment of the threshold is stopped, and the i-th class domain block C_{Di} is determined. Finally, m classes of domain blocks$C_{D1}, C_{D2}, \ldots, C_{Dm}$ are obtained. After getting domain block class, we also classify range blocks. According to above steps of finding the initial cluster center, class centers $c_1, c_2, \ldots c_m$ for m classes of domain blocks are obtained. Calculate the Euclidean distance between range block R_n and each class center $c_1, c_2, \ldots c_m$ select the class with the smallest distance to perform a matching search, and obtain corresponding m class of range blocks $C_{R1}, C_{R2}, \ldots C_{Rm}$. In this way, each class of range blocks only needs to perform matching search in the same class of domain blocks, for example, the m[th] range block class C_{Rm} and the m[th] domain block class C_{Dm} is matched. The matching process between different classes of range blocks is performed independently. Reduction of matching range effectively reduces encoding time.

The following are specific steps of classified MRI image compression algorithm:

Input: continuous m-layer MRI image $\{F_1, F_2, \ldots, F_m\}$.

Output: Fractal encoded file d_x, d_y, t, s, o}.

Stage 1: Fetch the consistent m-layer images {F_1,F_2,… ,F_m} in MRI image cuts, and consolidate them into one enormous image lattice F for compression. Split F into N X N run hinders that don't cover one another.

Stage 2: In a window of 2N x 2N, a stage size δ catches space blocks along F. Therapist area hinders and perform eight equidistant transforms.

Stage 3: According to above technique, area blocks are classified, and the comparing class of range blocks is gotten.

Stage 4: Take a range block R_i from the p^{th} class of range squares and take a space block D_j from the p^{th} class of area blocks. Figure s and o as indicated by (2) and (3), until all area blocks in the p^{th} class are completely looked, find the best coordinating square of range block R_i.

Stage 5: All range space classes are coordinated with their comparing area block classes, and fractal codes of nonstop m layer image are acquired.

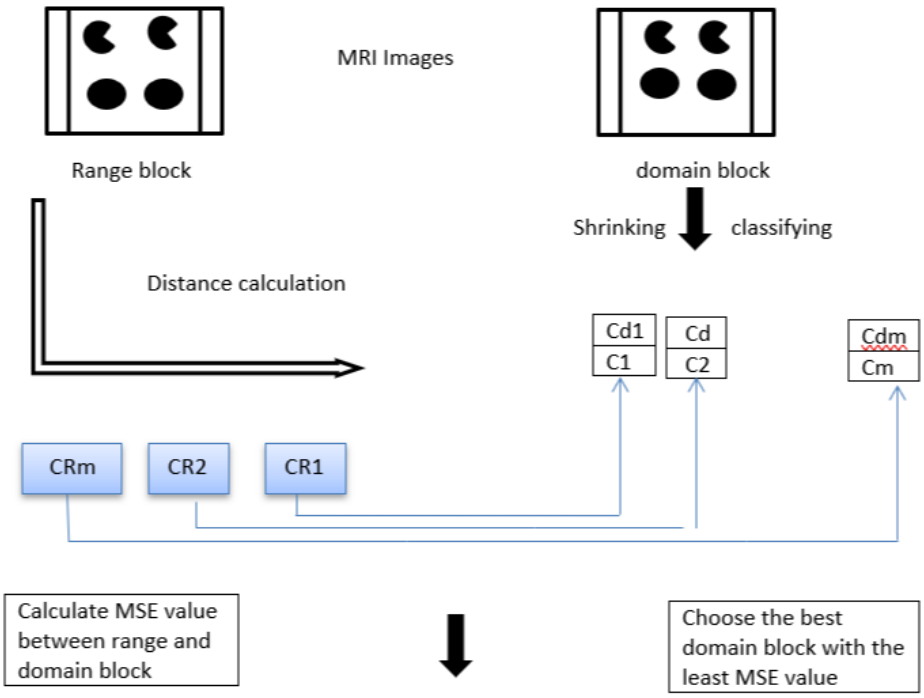

Fig.2. Flow chart of classified MRI image compression

2.3.2. Residual Compensation Mechanism

It is evident that the reproduced image is strongly linked to the source image due to the fact that the rebuilt image after lossy compression contains significantly more information. The restored image and the leftover image are not random clamor. The following condition is the basis for learning waiting image in this paper.

$$r(x, y) = f(x, y) - g(x, y)$$

where r (x, y) is the pixel evaluation of the old image, f (x, y) is the pixel assessment of the new image, and g (x, y) After the primary image is gigantically compressed, the extra image is found looking for return on investment. On the better edge, a Huffman coding depending on a whole number squared quantization is performed. The received code stream data is sent along with the first coded data, completing the Huffman coding of the return on original capital investment area.

The following are specific steps of the residual compensation mechanism algorithm:

Information: Original image and recreated image.

Output: Residual code document.

Stage 1: Calculate the remaining image.

Stage 2: Retain the significant coefficient of the limit under a specific quantization edge and create a fundamental image to discover the ROI area of the rest of the coefficient.

Stage 3: Huffman coding encodes a better whole number squared quantization limit for the ROI district.

Stage 4: The got code stream information is sent after the first coded information.

3. DWT (Discrete Wavelet Transform)

A wavelet transform rotates a pointer into its sub-band section of non-uniform information move limit. The Fourier transform applies to both continuous and discrete signals. The wavelet expansion shows a collection of limits. The sign, scaling limits, and wavelets are discrete in time. One is for the check (lowpass channel), and the other is for the picture information (high-pass channel). Two segment usages of one-dimensional breaking down in the straight and inverse rules complete the 2D DWT. With the use of the low and high pass channels, the image can be divided into three parts: even high-pass (HL), vertical high-pass (LH), and crosswise high-pass (HH) (LL). The rot method is then repeated on the low-pass sub-image LL to create the crumbling level. The imaginative image is decomposed into ten sub-images: LL3, (HLi; LHi; HHi), I 14 3; 2; 1, where LL3 is the most lowered objective low-pass sub-image at layer 3 of the chain of command of authority.

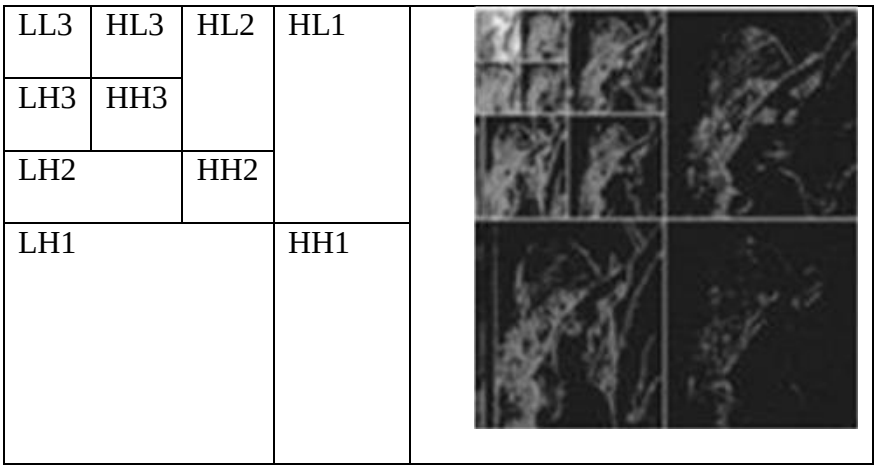

Fig.3. Applying DWT for three levels

The DWT transformation equation:

$$f(u,v) = \frac{2c(u)c(v)}{N} \sum_{m=0}^{N-1} \sum_{n=0}^{N-1} f(m,n) cos\left(\frac{2m+1}{2N} ux\right) cos\left(\frac{2n+1}{2n} VX\right)$$

Where u=0,1,2……N-1, v=0,1,2……N-1

Where c(k)=$\sqrt[1]{2} for k = 0$ =1 otherwise

3.1. DCT (Discrete Cosine Transform)

DCT enables segmentation of images into portions (or atypical subgroups) (in regards to the photos visual quality). DCT encapsulates a data center's optimal course of action in cosine bounds that fluctuate at infrequent intervals. For instance, lossy audio (MP3) and image (JPEG) compression, heinous ways for computing the mathematical key to insufficient differential situations, and so forth. Compression requires the use of cosine limits rather than sine limits since fewer cosine limits are required to assess a normal sign, but cosines imply a separate edge structure choice in differential scenarios. As with the discrete Fourier transform (DFT), a DCT translates a signal or image between spatial regions. Each square of a picture is compressed during quantization. The compressed chunks of the image are stored in a fundamentally degraded quantity of hole.

The 2D-DCT transformation equation:

$$c(u,v) = D(u)D(v) \sum_{X=0}^{N-1} \sum_{y=0}^{N-1} f(x,y) cos[(2x+1)\, u\pi/2\, N] cos(2y+1)\, v\pi/2\, N$$

Where, u, v, =01,23……N-1

The inverse 2D-DCT transformation equation:

$$f(x,y)\sum_{x=0}^{N-1}\sum_{y=0}^{N-1}D(u)D(v)D(u,v)cos[(2x+1)\,u\pi/2\,N]xcos[(2y+1)\,v\pi/2\,N]$$

Where D(u) =(1/N) ^1/2 for u=0

D(u) = 2(/N) ^1/2 for u=0,1,2,3…….... (N-1)

4. Experimental Results and Analysis

Examinations are conducted on a personal computer equipped with an Intel Core i5-4590 CPU and 12GB of memory. Matlab2016a is the operating system. The ADNI educational assortment's MRI picture groups are used as models, and the image size is 160 192 192, 8 pieces/pixel. The educational list is depicted in Table 1. From two perspectives, we compare the proposed calculation to conventional fractal MRI image compression. They are a combination of single-layer and persistent layer picture compression. Additionally, this paper's calculation is distinct from the BWT–MTF calculations. In these investigations, the size of the reach block is set to 4 4, the size of the region block to 8, and both the even and upward development are set to 8. By registering PSNR, we determine the nature of the decoded image. The (PSNR) is a logarithmic evaluation of the mean squared error (MSE) between the original image and the decoded image near with (2n1)2, where 2n 1 refers to the dark level limitation with the greatest distance. n denotes the number of pieces in a pixel. The higher the PSNR value, the less contortion is dealt with. Similarly, assessment pointers connect the compression time (T), the speedup percentage (SR), and the compression percentage (CR).

1) PEAK SIGNAL TO NOISE RATIO (PSNR) INDICATOR

In PEAK SIGNAL TO NOISE RATIO (PSNR) indicator, where n is the number of pixels for the image. X_i and Y_i represent gradation values of the i^{th} pixel for images X and Y, respectively.

2) SPEEDUP RATIO (SR) INDICATOR

$SR = \frac{T_S}{T_C}$ Where T_S is the time required to adopt traditional fractal MRI image compression method. T_C is the time required for the method in this paper.

3) COMPRESSION (CR) INDICATOR

$$CR = \frac{160x192x10}{Hx(8+8+3+8+3)}$$

Where, H is the number of range blocks. {8,8,3,8,3} represents the quantization level of fractal parameters $\{x_i, y_i, t_i, s_i, o_i\}$, respectively, which is the memory required to save these parameters.

4.1.1. Comparison for Continuous Layer of MRI Images

Each MRI image has four layers compressed. Calculate the average compression time and PSNR for each layer. The first image cut is 160192 pixels wide, the reach block is 44 pixels wide, and division gives 4048 area blocks.

The region block is 88 bytes, the level and upward development blocks are both 8, and division yields 2024 blocks of space.

Region blocks can be categorised into three sorts based on their spatiotemporal proximity to one another. There are three types of go squares. As shown in Table 2, the restored image for each of the three MRI images was compressed and decompressed using both the traditional and innovative fractal encoding methods. [average T(s), normal PSNR (dB)] To the human sight, the reconstructed image is not unfathomably distinctive, as illustrated in Tables 1 and 2. It also reduces coding time and PSNR when compared to conventional fractal coding.

Because the technique identifies all picture blocks initially, the typical method uses global pursuit. In addition to the three types of reach and space blocks, Speed should be adequate on multiple occasions. Due to the classification's volatility, the real speed gain is minimal.

4.1.2. Comparison for MRI Images with Residual Compensation Mechanism

Compressing the first four MRI layers. The four layers of photographs are combined and compressed by combination approach. Global domain and range block classification is also done.

Image Name	Screening	Complete 1Yr	Complete 2 YR
Uncompressed	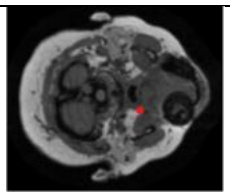	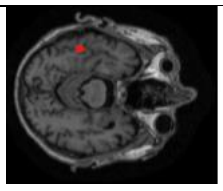	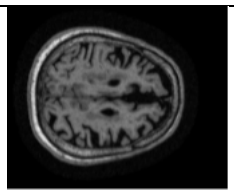

The proposed Algorithm	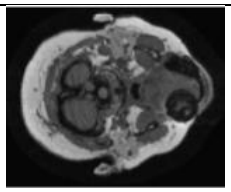	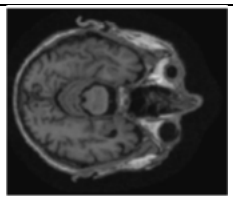	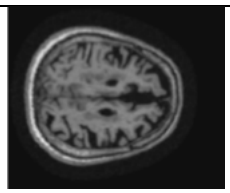
The BWT-MTF algorithm	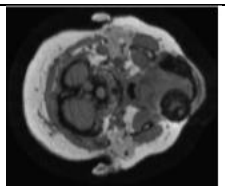	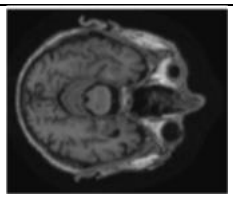	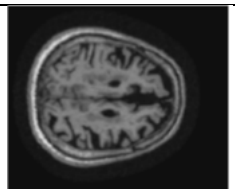

Table 1. Comparison data of decoding quality and performance for the algorithm

Method	Screening		Complete 1Yr		Complete 2Yr	
	T	PSNR	T	PSNR	T	PSNR
Traditional	29.02	23.42	27.92	24.72	27.04	27.63
Proposed	10.52	25.86	10.39	28.25	10.52	27.15

Table 2. Comparison for performance of traditional algorithm and proposed algorithm

4.1.3. Comparison between the Proposed Algorithm and BWT–MTF Algorithm

The 'codebook' is expanded from a single layer to a 4-layer image, improving organisation. This is followed by fractal coding with added compensatory framework. After merging, space squares and reach blocks are separated into ten groups.

Tables show that the suggested calculation with extra compensation segment produces excellent image quality. Despite the fact that its compression time is longer than the recommended computation without leftover compensation framework, its PSNR is the highest of the three.

When four layers of MRI pictures are combined and crammed, the time is multiplied. Regardless, all reach and area blocks are now isolated into 10 classes, allowing for more speed. Moreover, RCM enhances the character of the recreated image.

It should fairly compensate for the initial tragedy. The BWT-MTF technique compresses medical images utilising Huffman coding and hybrid fractal coding.

Method	Screening		Complete 1Yr		Complete 2Yr	
	T	PSNR	T	PSNR	T	PSNR
Traditional	161.16	23.42	171.61	24.72	161.42	27.69
Without RCM	44.50	26.86	42.02	25.62	40.10	27.51
With RCM	45.32	33.38	46.34	34.09	48.62	37.28

Table 3. Comparison for decoding quality of three algorithms

The Burrows-Wheeler (BWT-MTF) compression method is utilised to find the analytic highlight region, which is subsequently encoded with little loss of indicative quality. This method incorporates a fractal code using half-breeds. The coding sections are finally reassembled. The results of Tables 3 and 4 demonstrate the link between removing errors and overall product performance for the paper calculation and the BWT-MTF approach.

	Method	T	PSNR	CR	SR
Screening	proposed	2182	40..24	43.57	2.64
	BWT-MTF	1705	34.11	4.02	
Complete 1Yr	Proposed	2431	40.72	4.97	2.42
	BWT-MTF	1012	35.23	4.54	
Complete 2Yr	Proposed	2472	45.10	4.31	2.31
	BWT-MTF	901	36.53	4.81	

Table 4. Performance Comparison for the Proposed algorithm and BWT-MTF algorithm

PSNR is the usual MRI clinical image incentive. Due to the 192 layers in each MRI image, this is the hard and fast compression time Note that while the PSNR of Screening and Complete 2Yr are significantly improved, the compression proportion of Screening and

Complete 2Yr is reduced in Tables. Complete 1Yr has a higher compression ratio than BWT–MTF. The proposed technique's compression season is more pronounced than the BWT–MTF calculation's PSNRs for the three MRI images. It's a fractal compression flaw. Compression speed is increased by 2 to 10 times compared to standard calculation. Given the inconsistency of reach squares and area blocks, it is possible to distinguish between real and hypothetical speed gains.

5. Conclusion

Many new three-dimensional clinical data, such as MRI, CT, and three-dimensional ultrasound, have emerged with the advancement of clinical imaging. Due to the large number of three-dimensional clinical picture data, considerable storage and transmission costs are required. Clinical pictures are compressed so that less data needs to be transferred. Next, it is saved and then shared.

When compared to previous models, this newer design can both conserve space and improve transmission efficiency and transmission time. There is a major obstacle in clinical picture compression: increasing the compression ratio and decoding capability for packed images. We begin with the fact that the above three have been presented. In this light, we show how to apply a fractal-based MRI image compression technique. 2D progressive image is derived from a 3D MRI image. It is compressed using group fractal compression, which compresses pictures based on their grouping. Run squares and space blocks are spatiotemporally comparable, and that has classifiers assigned to it. In other words, in the case of a reach block, all you need to do is locate the best-plannable square in a region block.

To help speed up, let the limit on pool coordination to be reduced. Finally, a lossless MRI image compression method has been discovered. In terms of image quality, it was found that compared to the traditional fractal MRI image compression methods, the approach presented in this research provides faster compression, while preserving the original image. Despite the fact that PSNR (Peak Signal-to-Noise Ratio) is higher than BWT-MTF (BWT-Massachusetts Technology File - MTF), the compression ratio is not markedly poorer. This approach has been confirmed by proof. Then we must begin by working on it like this. One way to do this is to experiment with adding more subjects in the future. To enhance the security of the algorithm, it should be developed from the start in relation to its own compression calculation.

References

1. Bindu, P. V., and A. Jabeena. "Medical Image Compression: A Leap on Recent Progress and Publications." In *Advances in Automation, Signal Processing, Instrumentation, and Control*, pp. 2281-2289. Springer, Singapore, 2021.

2. Tahoces, Pablo G., J. Ramón Varela, María J. Lado, and Miguel Souto. "Image compression: Maxshift ROI encoding options in JPEG2000." *Computer vision and Image understanding* 109, no. 2 (2008): 139-145.

3. Zhang, Yudong, Zhengchao Dong, Lenan Wu, and Shuihua Wang. "A hybrid method for MRI brain image classification." *Expert Systems with Applications* 38, no. 8 (2011): 10049-10053.

4. Hosseini, Seyed Morteza, and Ahmad-Reza Naghsh-Nilchi. "Medical ultrasound image compression using contextual vector quantization." *Computers in biology and medicine* 42, no. 7 (2012): 743-750.

5. Sophia, P. Eben, and J. Anitha. "Implementation of region based medical image compression for telemedicine application." In *2014 IEEE international conference on computational intelligence and computing research*, pp. 1-4. IEEE, 2014.

6. Kaur, Manpreet, and Vikas Wasson. "ROI based medical image compression for telemedicine application." *Procedia Computer Science* 70 (2015): 579-585.

7. Schelkens, Peter, Adrian Munteanu, and Jan Cornelis. "Wavelet-based compression of medical images: Protocols to improve resolution and quality scalability and region-of-interest coding." *Future generation computer systems* 15, no. 2 (1999): 171-184.

8. Sridhar, K. V. "Implementation of prioritised ROI coding for medical image archiving using JPEG2000." In *2008 International Conference on Signals and Electronic Systems*, pp. 239-242. IEEE, 2008.

9. Hu, Min, Changjiang Zhang, Juan Lu, and Bo Zhou. "A multi-ROIs medical image compression algorithm with edge feature preserving." In *2008 3rd international conference on intelligent system and knowledge engineering*, vol. 1, pp. 1075-1080. IEEE, 2008.

10. Firoozbakht, Mohsen, Jamshid Dehmeshki, M. Martini, Yousef Ebrahimdoost, Hamdan Amin, M. Dehkordi, A. Youannic, and Salah D. Qanadli. "Compression of digital medical images based on multiple regions of interest." In *2010 Fourth international conference on digital society*, pp. 260-263. IEEE, 2010.

11. Bartrina-Rapesta, Joan, Joan Serra-Sagristà, and Francesc Auli-Llinas. "JPEG2000 ROI coding through component priority for digital mammography." *Computer Vision and Image Understanding* 115, no. 1 (2011): 59-68.

12. Agraftotis, D., David R. Bull, and Nishan Canagarajah. "Region of interest coding of volumetric medical images." In *Proceedings 2003 International Conference on Image Processing (Cat. No. 03CH37429)*, vol. 3, pp. III-217. IEEE, 2003.

13. Wang, Kaibin, and Aysegul Cuhadar. "Unbalanced 3-D tree structure for region-based coding of volumetric medical images." In *2006 International Conference of the IEEE Engineering in Medicine and Biology Society*, pp. 3286-3289. IEEE, 2006.

14. Sanchez, Victor, Rafeef Abugharbieh, and Panos Nasiopoulos. "3-D scalable medical image compression with optimized volume of interest coding." *IEEE Transactions on Medical Imaging* 29, no. 10 (2010): 1808-1820.

15. Nguyen, Binh P., Chee-Kong Chui, Sim-Heng Ong, and Stephen Chang. "An efficient compression scheme for 4-D medical images using hierarchical vector quantization and motion compensation." *Computers in biology and medicine* 41, no. 9 (2011): 843-856.

16. Sanchez, V. "Joint source/channel coding for prioritized wireless transmission of multiple 3-D regions of interest in 3-D medical imaging data." *IEEE Transactions on Biomedical Engineering* 60, no. 2 (2012): 397-405.

17. Elhannachi, Sid Ahmed, Nacéra Benamrane, and Taleb-Ahmed Abdelmalik. "Adaptive medical image compression based on lossy and lossless embedded zerotree methods." *Journal of Information Processing Systems* 13, no. 1 (2017): 40-56.

18. Yee, David, Sara Soltaninejad, Deborsi Hazarika, Gaylord Mbuyi, Rishi Barnwal, and Anup Basu. "Medical image compression based on region of interest using better portable graphics (BPG)." In *2017 IEEE international conference on systems, man, and cybernetics (SMC)*, pp. 216-221. IEEE, 2017.

19. Sridhar, K. V., and KSR Krishna Prasad. "Medical image compression using advanced coding technique." In *2008 9th International Conference on Signal Processing*, pp. 2142-2145. IEEE, 2008.

20. Prabhu, K. M. M., K. Sridhar, Massimo Mischi, and Halandur Nagaraja Bharath. "3-D warped discrete cosine transform for MRI image compression." *Biomedical signal processing and control* 8, no. 1 (2013): 50-58.

21. Bhavani, Sridharan, and Kepanna Gowder Thanushkodi. "Comparison of fractal coding methods for medical image compression." *IET image Processing* 7, no. 7 (2013): 686-693.

22. Juliet, Sujitha, Elijah Blessing Rajsingh, and Kirubakaran Ezra. "A novel medical image compression using Ripplet transform." *Journal of Real-Time Image Processing* 11, no. 2 (2016): 401-412.

23. Zhang, Yu-Dong, Yongyan Jiang, Weiguo Zhu, Siyuan Lu, and Guihu Zhao. "Exploring a smart pathological brain detection method on pseudo Zernike moment." *Multimedia Tools and Applications* 77, no. 17 (2018): 22589-22604.

24. Juliet, Sujitha, Elijah Blessing Rajsingh, and Kirubakaran Ezra. "A novel image compression method for medical images using geometrical regularity of image structure." *Signal, Image and Video Processing* 9, no. 7 (2015): 1691-1703.

25. Selvi, S. Arunmozhi, T. Ananth Kumar, and R. S. Rajesh. "CCNN: A Deep Learning Approach for an Acute Neurocutaneous Syndrome via Cloud-Based MRI Images." In Handbook of Deep Learning in Biomedical Engineering and Health Informatics, pp. 83-102. Apple Academic Press, 2021.

26. Rajakumar, G., and T. Ananth Kumar. "Design of Advanced Security System Using Vein Pattern Recognition and Image Segmentation Techniques." In Advance Concepts of Image Processing and Pattern Recognition, pp. 213-225. Springer, Singapore, 2022.

27. Juliet, Sujitha, Elijah Blessing Rajsingh, and Kirubakaran Ezra. "Projection-based medical image compression for telemedicine applications." *Journal of digital imaging* 28, no. 2 (2015): 146-159.